Clim. Past, 9, 719–733, 2013
www.clim-past.net/9/719/2013/
doi:10.5194/cp-9-719-2013

Climate of the Past
Open Access

Potential and limits of OSL, TT-OSL, IRSL and pIRIR$_{290}$ dating methods applied on a Middle Pleistocene sediment record of Lake El'gygytgyn, Russia

A. Zander and A. Hilgers

University of Cologne, Institute of Geography, Cologne, Germany

Correspondence to: A. Zander (anja.zander@uni-koeln.de)

Received: 18 September 2012 – Published in Clim. Past Discuss.: 28 September 2012
Revised: 15 February 2013 – Accepted: 20 February 2013 – Published: 14 March 2013

Abstract. This study tests the paleomagnetic and proxy-data based Mid- to Upper Pleistocene sediment deposition history of Lake El'gygytgyn by applying different approaches of luminescence dating techniques on sediment cores taken from the centre of the 175 m deep lake. For dating polymineral and quartz fine grains (4–11 µm grain size range) were extracted from nine different levels from the upper 28 m of sediment cores 5011-1A and 5011-1B. According to the independent age model, the lowest sample from 27.8–27.9 m below lake bottom level correlates to the Brunhes-Matuyama (B/M) reversal. Polymineral sub-samples were analysed by infra-red stimulated luminescence (IRSL) and post-IR IRSL measured at 290 °C (pIRIR$_{290}$) using single aliquot regenerative dose (SAR) sequences. SAR protocols were further applied to measure the blue light optically stimulated luminescence (OSL) and thermally-transferred OSL (TT-OSL) of fine-grained quartz supplemented by a multiple aliquot approach. Neither low temperature IRSL measurements at 50 °C nor any OSL dating approach on quartz yielded reliable results. Deconvolution of their dose response curves revealed a pseudo-increase of the dose response curves and explains the observed underestimation. The pIRIR protocol applied to polymineral fine grains was the only luminescence technique able to provide dating results of acceptable accuracy up to ca. 700 ka when correlated to the existing proxy-data and paleomagnetic based age record. We present the potential and limits of the different dating techniques and a correlation of pIRIR$_{290}$ results with the proxy-data based age model.

1 Introduction

Luminescence dating is long established as a reliable tool to provide numerical chronologies for Upper Pleistocene sediments from numerous depositional environments. The event being dated by luminescence is the exposure of the mineral grains to sunlight prior to deposition and coverage. Most dating studies are based on quartz optically stimulated luminescence (OSL) applied on sediment archives of aeolian, fluvial or lacustrine origin. However, the use of quartz for OSL dating is typically limited to the last 100–150 ka because of saturation effects of the quartz luminescence signal with increasing dose. Thermally transferred OSL (TT-OSL) was proposed by Wang et al. (2006) to extend the age range of quartz and to provide quartz OSL dates for Middle Pleistocene sediments. The TT-OSL signal is measured after the depletion of the conventional OSL signal and a subsequent pre-heat, which is applied to induce the thermal transfer of charge. The TT-OSL signal has a saturation limit at least an order of magnitude higher than the fast component of the conventional OSL signal (Wang et al., 2007) but, in contrast to initial suggestions by Wang et al. (2006), it is considerably less light sensitive than the fast bleaching OSL component (Tsukamoto et al., 2008; Jacobs et al., 2011). Infrared stimulated luminescence (IRSL) of potassium-rich feldspars has the potential to extend the datable age range because dose-response curves of K-rich feldspars or feldspar dominated luminescence emissions of polymineral fine grains show a much higher saturation dose compared to quartz. But it has been known for several decades now that the IRSL signal can show anomalous fading (Wintle, 1973). This signal loss over burial time often gives rise to significant age

underestimation. Fading correction procedures have been developed (Lamothe and Auclair, 1999; Huntley and Lamothe, 2001) to correct for these underestimations but they are inapplicable at samples, in which dose response curves advance the saturation level. Recent studies (Thomsen et al., 2008; Buylaert et al., 2009; Li and Li, 2011) have presented a measuring protocol, in which a high temperature IRSL signal is measured at an increased temperature after a first IR shine down at low temperature. This pIRIR signal appears to be less prone to fading and is more stable than the low-temperature IRSL measured at 50 °C ($IRSL_{50}$) but has the same high saturation dose limits as the low temperature IRSL. These characteristics make this a method of great importance for dating Middle and Upper Pleistocene deposits and it has become the preferred protocol for feldspar dating if fading corrections are unreliable or not valid (Buylaert et al., 2012).

Just a few studies have focussed on luminescence dating of lake sediments from the Upper and Middle Pleistocene so far (e.g. Forman et al., 2007; Juschus et al., 2007; Lowick and Preusser, 2011; Lukas et al., 2012). This is probably due to the fact that such environments are afflicted with several complications. One important complication is the accurate estimation of the paleo-water content. This variable is the most crucial, because water attenuates external radiation and causes a lowering of the dose rate received by the dosimeters, i.e. the sediment grains. The dose rate is a substantial part of the age equation and faulty dose rate calculations lead to inaccurate ages. A second problem that can affect the dose rate determination in lacustrine environments is the presence of radioactive disequilibria in the uranium decay chain (Krbetschek et al., 1994). Similar to changes in water content, this imparts a non-constant dose rate on the sampled material through time. A third question that has to be considered comprises the potential sediment transport processes and remobilisation processes by turbidites or landslides.

An independent age model for a 3.6 Ma core composite of Lake El'gygytgyn is provided by magnetostratigraphy and tuning of proxy-data to the regional insolation and global marine isotope stratigraphy (Melles et al., 2012; Nowaczyk et al., 2013). The objective of our study was to provide complemental information on the core stratigraphy by applying luminescence dating techniques and to analyse the potential and limits of four different dating techniques, applied on an – in terms of the dating range of luminescence techniques – exceptionally old sediment record.

Two comprehensive luminescence dating studies on drilling cores from Lake El'gygytgyn were already published by Juschus et al. (2007) and Forman et al. (2007). They applied a SAR-IRSL protocol and a multiple aliquot additive dose IRSL protocol, respectively, on polymineral fine grain samples from the upper ∼ 12 m, i.e. 200 ka, of the sediment record and report good agreement with the age model down to about 160 ka. In our study, the focus is placed on the sediment record from 6–31 m below lake floor, i.e. 145–757 ka (Melles et al., 2012; Nowaczyk et al., 2013).

2 Site information

Lake El'gygytgyn is located in Central Chukotka, NE Russia (67°30′ N, 172°0530′ E, 492 m a.s.l., Fig. 1), ∼ 100 km north of the Arctic Circle. It was formed about 3.58 Ma ago by a meteorite impact in Upper Cretaceous volcanic rocks of the Okhotsk-Chukchi Volcanic Belt (OCVB) (Gurov et al., 2007).

The climate in Chukotka can be characterized as cold, dry and windy with mean winter temperatures between −32 °C and −36 °C in January and mean summer temperatures between +4 °C and +8 °C in July/August (Treshnikov, 1985). Today the surface of the roughly circular lake with a diameter of ∼ 12 km and a maximum water depth of 175 m (Nolan and Brigham-Grette, 2007; Melles et al., 2007) is frozen and covered with ice for about 9 months of the year from mid October until early to mid July (Nolan et al., 2002; Melles et al., 2012). Fluvial and aeolian input is hence limited to the few summer months when the lake surface is open water and the light conditions most likely allow a reasonable bleaching of the sediment grains. During the ice covered season, the water column is thermally stratified but by late summer after the ice break up, it becomes fully mixed (Nolan and Brigham-Grette, 2007). The fluvial input to the lake is low and much of the sediment is deposited at the mouth of the inflows in shallow lagoons, which are dammed by gravel bars formed by wave and lake ice action (Melles et al., 2011). Temporary deposition in these lagoons and further transport through the clear surface waters, giving a Secchi transparency depth of 19 m in summer (Melles et al., 2012), are thought to enable a reasonable bleaching of the suspended matters.

The bedrock of the Lake El'gygytgyn catchment consists of ignimbrites, tuffs and andesite-basaltes associated with the Pykarvaam, Voron'in, Koekvun' and Ergyvaam formations (Nowaczyk et al., 2002). The sediments in the central part of the lake consist mainly of clay and silt with some very small quantities of fine sand and the mineral composition is dominated by a mixture of quartz, feldspars (K-feldspar and plagioclase) and clay minerals. Although the bedrock samples of the catchment contain fairly scattered amounts of quartz between 3 % and 27 %, surface samples of the southern and south-eastern shore show a fairly homogenous enrichment of up to 34 % quartz (Wennrich et al., 2013). The enrichment of quartz is associated with the silt fraction and is explained by cryogenic weathering processes within the active layer of the permafrost in the lake surroundings (Schwamborn et al., 2008, 2012). The sediments of the central basin contain 26 % quartz, 21 % plagioclase, 6 % K-feldspar, 2 % calcite, 10 % illites, mica and other phyllosilicates and heavy minerals (Wennrich et al., 2013). Most of the mineral concentration values fit within the concentration range of the inlet stream

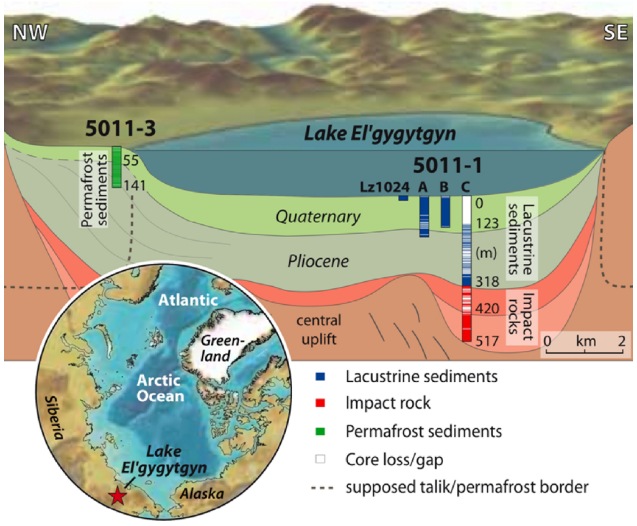

Fig. 1. Location of Lake El'gygytgyn in northeastern Russia (inserted map) and schematic cross-section of the El'gygytgyn basin stratigraphy showing the location of ICDP Sites 5011-1 and 5011-3. Lz1024 is a 16 m long percussion piston core taken in 2003 that fills the stratigraphic gap between the lake sediment surface and the top of drill cores 1A and 1B (from Melles et al., 2012).

sample composition and the bedrock composition. A local component consisting of weathering products of the source rocks transported as suspended load, mass movements or debris flows from the shelf to the central basin is thus very likely (Juschus et al., 2009; Niessen et al., 2007). Though, a certain long distance aeolian transport component in the sediments is also likely with regard to the prevailing northern and southern wind directions (Nolan and Brigham-Grette, 2007). In consequence, the feldspar and quartz minerals used for analyses in this study most likely represent a mixture of local fluvial and lacustrine, re-deposited and long distance transport minerals. A comprehensive study about the climatic and environmental history of Lake El'gygytgyn is given in Melles et al. (2007).

The samples of this study originate from cores A and B of ICDP site 5011, which was drilled from February until April 2009 employing a 100 tons drilling platform on the artificially thickened ice cover in 170 m water depth in the central part of Lake El'gygytgyn (Melles et al., 2011; Fig. 1).

3 Sample preparation

The cores from ICDP site 5011 were taken in transparent plastic liners of 6.6 cm diameter. For luminescence dating, 10 cm thick pieces were taken from replicate core parts and wrapped with black tape to prevent further light exposure. These liner pieces were opened under subdued red-light conditions and a small block of $3 \times 3 \times 6$ cm was cut out of the inner core to exclude any grains that were exposed to light during cutting and preparing of the liner pieces. The small block was then treated with hydrochloric acid, hydrogen peroxide and sodium oxalate to remove carbonate, organics and dissolve coagulations. The samples showed no chemical reaction to hydrochloric acid but some of the samples showed a medium reaction to hydrogene peroxide, indicating an at least perceivable organic content. Due to the lack of sufficient sand-sized minerals, the 4–11 µm fine grain fraction was prepared following Frechen et al. (1996). Quartz was separated by etching the polymineral fine grains with hexafluorosilicic acid for seven days.

The remaining sediments from the liner were dried, homogenised and prepared for gamma-ray spectrometry. The effective water content was determined by weight loss after drying the bulk samples and is given in relation of weight water to dry mass. Comparing the results with the original water content, measured at a second correlative core soon after drilling, most of the values are in fairly good agreement (Table 1), indicating that no significant water loss has happened between coring and sample preparation. Only sample 1A1H3, taken from a turbidite layer, shows a significant discrepancy.

4 Dosimetry

Radionuclide analyses (uranium, thorium, potassium) were carried out by low-level gamma-ray spectrometry in the Cologne laboratory and at the VKTA Rossendorf e.V. (D. Degering, Dresden), respectively (Table 1). Between 70 g and 157 g of dry sample material was packed in polystyrol containers and stored for at least four weeks to compensate for radon loss induced by sample preparation.

In water-lain sediments disequilibria in the uranium decay series are common (Krbetschek et al., 1994), though they are often related to the presence of carbonates or organic matter. Weathering and alteration processes are also capable to withdraw nuclides of the uranium decay chain from the sedimentary system and enable a selective accumulation or degradation under suitable conditions (Kemski et al., 1996). Changes of the sediment dose rate over burial times have an impact on age estimates but they are hardly quantifiable over large time scales. The Cologne gamma-ray spectrometer has a good sensitivity in the higher energy part of the spectrum and ^{238}U is hence quantified by peaks of ^{226}Ra, ^{214}Pb and ^{214}Bi, emitting gamma radiation beyond 100 keV. The high resolution gamma-spectrometer in Dresden is in addition sensitive in the lower energy spectrum and can quantify ^{234}Th, which directly follows the mother isotope ^{238}U and has its main emissions at 63 and 93 keV. Comparing ^{238}U/^{234}Th with ^{226}Ra provides information about disequilibria in the early decay chain and can reveal uranium loss or uptake since uranium is mobile in oxidising aqueous solutions. The samples analysed in Dresden show no significant differences between ^{238}U/^{234}Th and ^{226}Ra but two of the

Table 1. Results of dose-rate determination using high-resolution gamma-ray spectrometry. Samples marked with an asterisk were measured at the VKTA Rossendorf e.V. The other 5 samples were measured at the luminescence laboratory in Cologne. Water content 1 was measured by drying the bulk sediment finally used for dose rate measurements and water content 2 was measured at a second correlative core soon after drilling. Water content 2 was later used for age calculations. All water content values are quoted as weight water/weight dry sediment. All values are presented with their 1-sigma error.

Lab. Code	Sample ID	Composite depth (m)	Field depth (m)	Water content (weight-%) 1	Water content (weight-%) 2	U (ppm)	Th (ppm)	K (%)
C-L3111	1A1H2	6.487–6.587	3.76–3.86	90.3	94.7	3.36 ± 0.18	12.40 ± 0.72	2.42 ± 0.09
C-L3112	1A1H3	7.469–7.569	4.77–4.87	30.9	79.0	3.33 ± 0.17	12.13 ± 0.70	2.34 ± 0.09
C-L2843	1B2H2*	11.09–11.19	8.32–8.42	72.5	52.9	4.30 ± 0.30	11.80 ± 0.40	2.39 ± 0.08
C-L3113	1A3H1	11.694–11.794	8.88–8.98	45.0	42.8	2.47 ± 0.13	10.46 ± 0.60	1.94 ± 0.08
C-L3114	1A3H2	12.596–12.696	9.815–9.915	69.3	74.8	3.08 ± 0.16	12.32 ± 0.71	2.42 ± 0.09
C-L3115	1B3H2	14.169–14.269	11.319–11.419	66.0	67.4	2.85 ± 0.15	11.75 ± 0.68	2.24 ± 0.09
C-L3116	1A4H2	15.626–15.726	12.79–12.89	73.8	70.5	6.17 ± 0.32	13.21 ± 0.77	2.53 ± 0.10
C-L2844	1A6H1B*	20.869–20.969	17.88–17.98	59.2	61.0	4.20 ± 0.30	12.40 ± 0.40	2.45 ± 0.08
C-L2845	1A9H2*	31.05–31.15	27.817–27.917	67.2	61.5	3.90 ± 0.40	12.70 ± 0.40	2.49 ± 0.08

three samples show slightly lower values for ^{210}Pb compared to ^{226}Ra (Fig. S1 in the Supplement). This gives evidence for the uranium series not being completely in the state of equilibrium, but with regard to the decay rates of the short life nuclides behind ^{226}Ra, the difference can be attributed to mobilisation processes within the last about 100 yr and thus can be neglected in dose rate calculation for luminescence dating. For all the three samples analysed here, the activities of the daughters ^{226}Ra and ^{210}Pb still agree within 2-sigma errors with the activity of the mother (Fig. S1 in the Supplement). Hence, the impact on age calculation is marginal. Regarding the dose rates calculated for this study, an underestimation of about 1 ppm Uran would result in age overestimations of about 6 to 8 % which is covered by the uncertainty range of the dating result. Several studies have dealt with comparably more significant Uranium disequilibria in marine coastal sediments, cave sediments and peat sediments (Zander et al., 2007; Guibert et al., 2009; Preusser and Degering, 2007). They calculated ages for different modelled Uranium uptake scenarios in open and closed systems and found good agreement with independent age control and only little effect on the resulting age estimate.

Dose rates (Tables 3 and 6) and ages were calculated using the "age" software (version 1999) by R. Grün, Canberra, which includes the dose conversion factors published by Adamiec and Aitken (1998). Alpha efficiency was set to 0.035 ± 0.02 for quartz samples and 0.07 ± 0.02 for polymineral fine grain samples (Rees-Jones, 1995; Mauz et al., 2006; Frechen and Schirmer, 2011).

Attenuation factors and water content

The cosmic contribution to the dose rate is usually calculated according to the sampling depth. It can be neglected for the given samples, because the influence of cosmic radiation on the minerals is completely attenuated by overlying sediment and water column. More important is the impact of the sediment water content. Attenuation of ionising radiation is more effective in sediments with water-filled interstices and has strong effects on resulting age estimates. The "as found" water contents are hardly representative for the moisture conditions during the time span of burial, especially not for such a long period of time as considered in this study. Mechanical compaction by overlying sediments and mass movements may have reduced or increased the water content during burial times and are difficult to quantify. Lowick and Preusser (2009) have presented a complex method to quantify full water saturation of sediments, though a simple experiment was carried out in our study to get a rough estimate about the maximum water capacity. Sample material extracted from the core liner and with no further mechanical treatment was dried at 105 °C for 1 day and filled in beakers with a perforated bottom. The beakers were placed in a 1 cm water column for 1 day allowing a total soaking of the sample material. Maximum water contents measured immediately after removing the samples from the water were between 118 % and 131 % in relation to dry mass. The "natural" water contents measured at the core are slightly lower, ranging between 95 % for the upper sample and 43 % as a minimum value. The difference can probably be attributed to sediment compaction and drainage by sediment upload under natural conditions. There is a small trend visible down the record as observed by Juschus et al. (2007). They presented similar water contents between 90 % and 50 % for the upper 17 m of core LT1024 and calculated three different dose rates for each sample with different water content scenarios. Only the upper few dm of the core were over-saturated showing water contents of up to 190 %. Water contents of core PG 1351 presented by Forman et al. (2007) decrease from about 70–80 % down to 30–40 at 800–900 m depth. They added 5 % to the moisture content for age calculation to reflect an earlier history of wetter conditions. It is fact that a retrospective determination of water content changes through time is far from being straightforward. We therefore took the measured

water content for age calculation and added three more age estimates calculated with fictive water contents in the tables to illustrate the impact of water content variation on age calculation (Tables 3 and 6).

5 Luminescence measurements

Luminescence measurements were carried out on an automated Risø TL/OSL Reader (TL-DA 12) with a calibrated ^{90}Sr/^{90}Y beta source delivering 4.08 Gy min^{-1}. An U340 filter was used for quartz measurements and an interference 410 nm filter for IRSL measurements on polymineral samples. Several different dating techniques were applied in this study to evaluate the most appropriate protocol for achieving reliable luminescence age estimates for such old, i.e. $>$ 300 ka, sediments (Table 2). This expanded dating programme evolved from the fact that the sediments analysed here are comparably old and cover a time span which is not often securely dated by luminescence techniques.

5.1 SAR-OSL on fine grain quartz

The standard SAR protocol (Murray and Wintle, 2000) was applied on three samples, using blue stimulation for 50 s at 125 °C, a pre-heat of 240 °C and a cut heat of 220 °C. Equivalent dose (D_e) values were determined using the first 0.6 s of the OSL decay curve, and subtracting the background of the last 5 s. Another approach using the early background (EBG) subtraction method (Ballarini et al., 2007) with an integral of 0–0.4 s for OSL-signal determination and a background integral of 1.0–1.4 s, as described by Lowick and Preusser (2011), did not improve the dataset and was therefore rejected. The EBG subtraction did not change D_e-values compared to those using a late background (LBG) subtraction but only reduced the signal intensity and increased uncertainties. This suggests that the OSL signal is dominated by the fast component for which the SAR protocol was designed (Wintle and Murray, 2006). Dose response curves were fitted with a single exponential plus linear function (SEPL). An experimental dose-response curve measured for sample 1B2H2 with 12 dose steps up to a 1237 Gy fitted well to a SEPL function and did not show any saturation effects (Fig. 2). Validation of the protocol parameters was verified by preheat plateau tests and dose recovery tests at different temperatures. The validation tests both confirmed an appropriate pre-heat temperature between 220 °C and 240 °C and a perfect dose recovery at 240 °C with a measured to given dose ratio of 1.00 (Fig. 3a and b). IR tests for feldspar contamination were made standard practice.

5.2 Thermally transferred OSL (TT-OSL)

The simplified SAR protocol for TT-OSL developed by Porat et al. (2009) (Table 2) was tested on 3 different samples. A dose recovery test carried out on 1A3H1 failed to meet the validation criteria; the average measured dose overestimated the given dose by more than 25 % and resulted in a ratio of 1.32. The recycling ratio was poor (more than the acceptable 10 % deviation) and the recuperation of 10–20 % was significantly exceeding the acceptance level of 5 % (Murray and Wintle, 2000). An additional hot bleach (OSL shine down at 300 °C for 100 s), as proposed by Stevens et al. (2009), was then added after the TT-OSL measurement to remove the residual charge carried over from the regenerated dose measurements to the test dose measurement cycle. This lead to a perfectly linear dose response curve (Fig. 4), however, the overestimation was hardly reduced, the recycling ratio remained poor, and the recuperation still varied between 4 % and 10 %. To avoid the problem of charge transfer, a multiple aliquot regenerative dose (MAR) TT-OSL approach was designed and tested. Twelve and 16 discs, respectively, were prepared from two samples (Table 3). The natural OSL and the natural TT-OSL (step 2–5 from the given SAR protocol, Table 2) were recorded and followed by a hot bleach (300 s blue stimulation at 280 °C). The same discs were then irradiated with 4 dose steps up to 814 Gy and step 2–5 from the SAR protocol were repeated. The first 0.4 s of the natural TT-OSL signal were used for short shine normalisation and the residual level was determined by repeating step 2–5 on the first three discs. D_e-values were determined by integrating the first 1.2 s and the average signal of the last 10 s was subtracted for background.

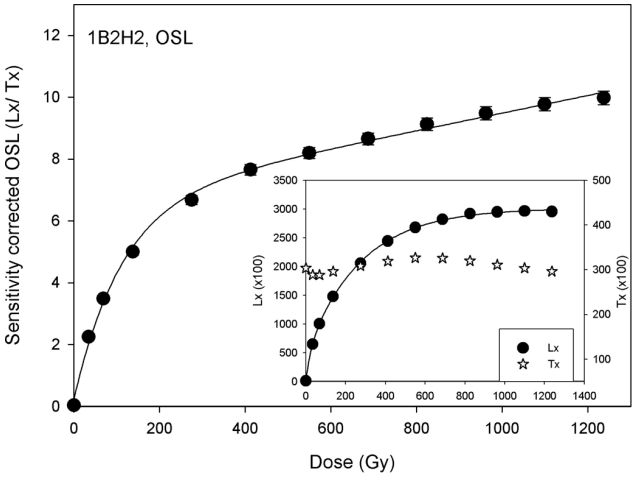

Fig. 2. Saturation dose curve of sample Elgy1B2H2 fitted to a single exponential plus linear function. The standard SAR protocol was applied with 12 dose steps up to a maximum beta dose of 1237 Gy. Up to about 400 Gy the dose response signal is best fitted to an exponential function and then beyond to a linear function up to 1237 Gy. The inset shows the deconvoluted L_x/T_x. The background subtracted OSL regenerative curve is in saturation but a decreasing test dose signal results in a linear increase of the dose response curve.

Table 2. Compilation of measurement protocols used in this study.

	OSL[a]	TT-OSL[b]	TT-OSL modified[c]	IRSL$_{50}$[d]	pIRIR$_{290}$[e]
1	Dose	Dose	Dose	Dose	Dose
2	Pre-heat (240 °C, 10 s)	Pre-heat (200 °C, 10 s)	Pre-heat (200 °C, 10 s)	Pre-heat (270 °C, 10 s)	Pre-heat (320 °C, 60 s)
3	OSL (125 °C, 50 s) → L_x	OSL (125 °C, 300s) → L_x	OSL (125 °C, 300 s) → L_x	IRSL (50 °C, 350 s) → L_x	IRSL (50 °C, 200 s) → $L_{x_{\mathrm{IRSL50}}}$
4	Test dose	Pre-heat (260 °C, 10 s)	Pre-heat (260 °C, 10 s)	Test dose	IRSL (290 °C, 200 s) → $L_{x_{\mathrm{pIRIR290}}}$
5	Pre-heat (220 °C, 0 s)	OSL (125 °C, 100s) → $L_{x_{\mathrm{TT}}}$	OSL (125 °C, 100 s) → $L_{x_{\mathrm{TT}}}$	Pre-heat (270 °C, 10 s)	Test dose
6	OSL (125 °C, 50 s) → T_x	Test dose	Heat (300 °C, 100 s)	IRSL (50 °C, 350 s) → T_x	Pre-heat (320 °C, 60 s)
7	Return to 1	Pre-heat (220 °C, 10 s)	Test dose	Return to 1	IRSL (50 °C, 200 s) → $T_{x_{\mathrm{IRSL50}}}$
8		OSL (125 °C, 100 s) → T_x	Pre-heat (220 °C, 10 s)		IRSL (290 °C, 200 s) → $T_{x_{\mathrm{pIRIR290}}}$
9		Heat (300 °C, 100 s)	OSL (125 °C, 100 s) → T_x		IRSL (325 °C, 100 s)
10		Return to 1	Heat (300 °C, 100 s)		Return to 1
11			Return to 1		

[a] after Murray and Wintle (2000), [b] after Porat et al. (2009), [c] after Stevens et al. (2009), [d] after Wallinga et al. (2000), [e] after Thiel et al. (2011).

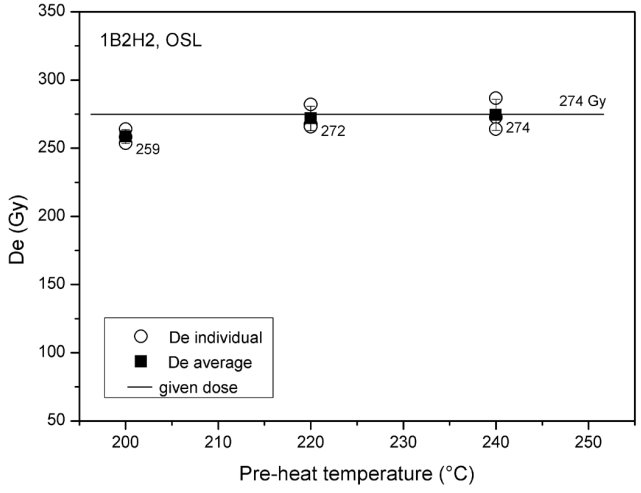

Fig. 3a. Validation of protocol parameters. A pre-heat plateau test at sample 1B2H2, carried out to define the appropriate pre-heat temperature. Three sub-samples of fine grain quartz were measured per temperature step and the resulting D_e plotted against the temperature. A 240/220 °C pre-heat/cut heat was chosen for further experiments with the SAR protocol.

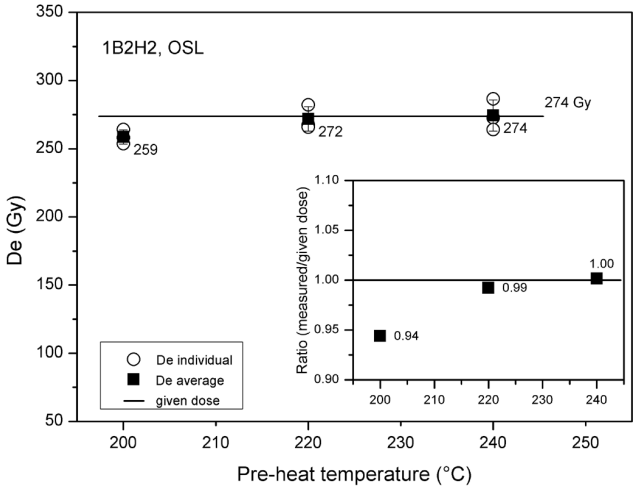

Fig. 3b. A dose recovery test combined with a pre-heat plateau for fine grain quartz. Samples were first bleached by a 100 s shine down at 125 °C to reset the natural luminescence signal and then irradiated with a 274 Gy beta dose. Three sub-samples each were measured at three different temperatures and yielded a perfect match at 240 °C with the given dose (ratio is 1.00, see inset), if the exponential plus linear function is fitted for D_e determination.

5.3 SAR-IRSL$_{50}$ on polymineral fine grain

The SAR-IRSL$_{50}$ protocol proposed by Wallinga et al. (2000) for coarse grain feldspars was applied on the polymineral fine grain fraction (Table 2). This fraction contains the natural fine silt mineral composition including quartz, though the IR stimulated luminescence emitted in the 410 nm range is dominated by potassium-rich feldspar. IRSL measurements were carried out for 350 s at 50 °C (IRSL$_{50}$) through an Oriel interference filter (410 nm, 5 mm thickness, 4.5 cm diameter). The first 18 s were used for D_e determination and the last 30 s subtracted as background. Dose recovery pre-heat plateau tests were conducted to determine the appropriate pre-heat temperature and to verify the protocol parameters. A set of 20 sub-samples of sample 1A1H2 received a hot bleach, i.e. a 100 s IRSL stimulation at 280 °C in the reader and a subsequent beta dose of 206 Gy. Four discs each were measured at different pre-heat temperatures using the same thermal treatments for the regenerative dose and the test dose. The average D_e's obtained for the different pre-heat temperatures show a D_e plateau between 210 and 290 °C and "measured to given dose" ratios between 1.04 and 1.01 (Fig. 5), confirming the applicability of the protocol. A pre-heat temperature of 270 °C was finally chosen for the SAR-IRSL dating protocol.

5.4 Post-IR IRSL (pIRIR$_{290}$) on polymineral fine grain

The pIRIR$_{290}$ protocol (Table 2) proposed by Thiel et al. (2011) for middle and upper Pleistocene loess from Austria was applied on eight polymineral fine grain samples. All sub-samples were prepared on aluminium discs and all measurements were made on a Risø TL-DA-12 with a Oriel

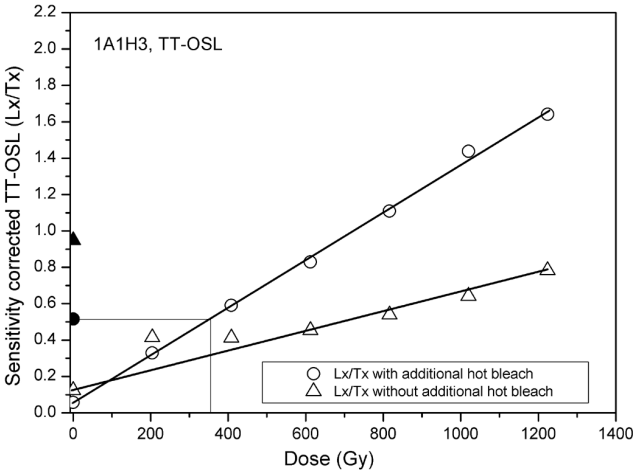

Fig. 4. Result of the modified SAR TT-OSL (applied to fine grain quartz) protocol after Porat et al. (2009) before (triangles) and after (circles) adding an additional hot bleach before the test dose measurement.

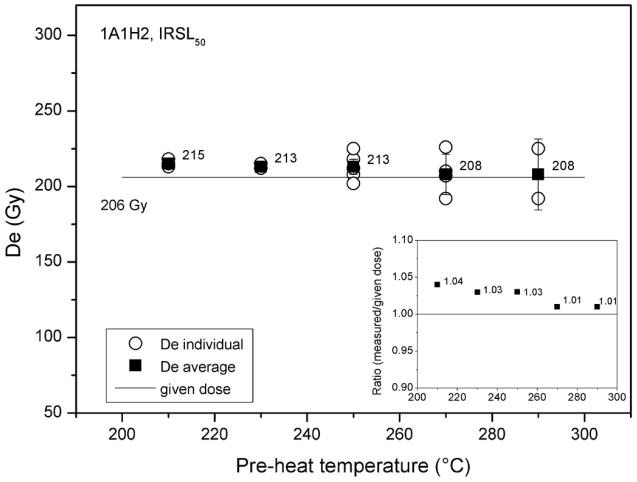

Fig. 5. Dose recovery pre-heat plot on sample 1A1H2 with the SAR-IRSL$_{50}$ protocol. Samples were first bleached by a 300 s shine down at 50 °C to reset the natural luminescence signal and then irradiated with a 206 Gy beta dose. Four sub-samples each were measured at five different temperatures and yielded a perfect match at 270 °C with the given dose (ratio is 1.01, see inset), if a single exponential plus linear function is fitted for D_e determination.

interference filter (410 nm, 5 mm thickness, 4.5 cm diameter). The first 2.4 s of the signal were used for D_e determination and the last 20 s were subtracted as background. With regard to the small number of sub-samples measured (Table 5), the median of the individual measurements was finally used as best representative for the average equivalent dose. In reference to the bleaching experiments, the signal left after bleaching for 3 h under natural sunlight (20 Gy) was subtracted from the pIRIR$_{290}$ D_e's (for discussion see also Thiel et al., 2011; Buylaert et al., 2012).

6 Results

6.1 SAR-OSL

The results obtained for the standard SAR-OSL protocol on quartz underestimate the expected age range significantly. Maximum D_e-values remained below 410 Gy and none of the three samples reached the saturation level. The maximum D_e was obtained for sample 1A6H1B. With regard to the age model provided by Melles et al. (2012) and Nowaczyk et al. (2013) sample 1A6H1B from 17.88–17.93 m b.l.f. (below lake floor) is supposed to be deposited about 465 ka ago. Sample 1A9H2 was taken between 27.817–27.917 m b.l.f. and is supposed to be 757 ka yr old. The SAR-OSL results of 137 ± 20 ka and 129 ± 13 ka for these two samples are far below the expected age range and show no increase in age with depth (Table 3 and Fig. 6). Although the dose response curves show no saturation effects with increasing dose, 400 Gy appears to be the maximum D_e for fine grain quartz. Thus, a quartz age beyond 200 ka is not attainable.

Although the SAR-OSL protocol is the most accepted protocol and has proved very successful when dating quartz, there are several studies reporting age underestimations for quartz beyond the Eemian or even as young as 70 ka (Murray et al., 2008). Similar observations were made by Lowick and Preusser (2011), Lowick et al. (2010), Lai (2010), Timar et al. (2010), who all reported on underestimations with fine grain quartz. The majority of these studies show that the samples meet the standard validation criteria for the SAR protocol, which usually allows the assumption to obtain reliable OSL ages. They all observed well-shaped dose response curves, which are best fitted to a SEPL function. While the characteristics of the dose response curve suggested that determination of D_e-values up to 400 Gy should be possible, Lai (2010) showed that age determination was only reliable up to 230 Gy. Lowick and Preusser (2011) and Lowick et al. (2010) reported on sedimentary quartz from northeastern Italy. Their OSL ages agree well with biochronological constraints up to 140 Gy (70 ka) but increasingly underestimate the age beyond this point. They assume that the underestimations are caused by the presence of different components of luminescence signals with different luminescence characteristics but have no real explanation for them. They also report on the slow growing dose response curve beyond 400 Gy, which is represented by a linear component. Chapot et al. (2012) have analysed this problem by comparing a natural dose response curve, which was constructed from the test dose normalized natural OSL signals of seven samples from a Chinese loess record, and the laboratory generated dose response curves (DRC). They observed a continuous increase of the laboratory generated normalized OSL signal above 500 Gy but no growth in the equivalent natural DRC at these

Table 3. SAR-OSL dating results and multiple aliquot regenerative dose (MAR) TT-OSL dating results obtained on fine grain quartz (4–11 µm). Ages and dose rates are given for different assumed and the measured water content (weight-%) to point out the significance of the water content on the age estimates. All analytical results are presented with their 1-sigma error.

Sample ID	Composite depth (m)	Protocol	Number of sub-samples	RSD	Mean recycling ratio	Mean recuperation (%)	D_e (Gy)
1B2H2	11.09–11.19	SAR-OSL	6	5.0	1.01	0.9	380 ± 23
1A6H1B	20.869–20.969	SAR-OSL	8	25.1	0.99	1.4	404 ± 47
1A9H2	31.05–31.15	SAR-OSL	7	5.8	1.00	2.9	376 ± 22
1A1H3	7.469–7.569	TT-OSL	16	–	–	–	408 ± 35
1A4H2	15.626–15.726	TT-OSL	12	–	–	–	485 ± 34

Sample ID	Expected age* (ka)	Protocol	OSL age (ka) Water content assumed for age calculation				Dose rate (Gy ka^{-1}) Water content assumed for age calculation			
			measured	50 %	70 %	90 %	measured	50 %	70 %	90 %
1B2H2	∼ 218	SAR-OSL	123 ± 13	121 ± 12	139 ± 15	158 ± 17	3.1 ± 0.3	3.1 ± 0.3	2.7 ± 0.2	2.4 ± 0.2
1A6H1B	∼ 465	SAR-OSL	137 ± 20	126 ± 18	146 ± 21	165 ± 24	2.9 ± 0.3	3.2 ± 0.3	2.8 ± 0.2	2.4 ± 0.2
1A9H2	∼ 757	SAR-OSL	129 ± 13	118 ± 12	136 ± 14	155 ± 16	2.9 ± 0.3	3.2 ± 0.3	2.8 ± 0.2	2.4 ± 0.2
1A1H3	∼ 168	TT-OSL	170 ± 21	139 ± 16	161 ± 19	182 ± 22	2.3 ± 0.2	2.9 ± 0.2	2.5 ± 0.2	2.2 ± 0.2
1A4H2	∼ 320	TT-OSL	151 ± 18	131 ± 15	151 ± 17	171 ± 20	3.2 ± 0.3	3.7 ± 0.3	3.2 ± 0.3	2.8 ± 0.3

* Inferred from Melles et al. (2012) and Nowaczyk et al. (2013).

doses. The divergence appears at about 150 Gy and defines the maximum limit of quartz OSL dating. They conclude that that D_e estimates above this value are likely to be underestimated. The available dataset of three SAR-OSL measurements of this study does not allow to construct a reliable natural DRC but the L_n/T_n values range between 3.6 ± 0.14 (1A9H2), 4.0±0.37 (1A6H2B) and 4.0±0.12 (1B2H2), indicating no increase with increasing natural dose, whereas the laboratory-generated dose response curve shows a constant increase up to 1240 Gy, as observed by Chapot et al. (2012) (see also Sect. 7).

A deconvolution of the L_x/T_x quotient from our study revealed an obvious answer to the question, why the dose response curve shows a linear response to high doses. Plotting the background-subtracted regenerated signals (L_x) and the background-subtracted test dose signals (T_x) against the administered beta dose shows a saturation of the L_x-curve above 400–500 Gy. The corresponding test dose signal (T_x) shows a small rise up to the 500 Gy regenerative dose and a decrease beyond, although the test dose was always kept constant (see inset Fig. 2). The ratio then seems to indicate a rising L_x/T_x with dose but the uncorrected OSL signal is in saturation. Hence, signal growth of the sensitivity-corrected OSL signals is an artefact of the response to the test dose that is commonly well below the saturation level. Here, sensitivity correction as conducted as part of the SAR protocol results in erroneous equivalent dose estimates in dose ranges beyond the saturation level of the uncorrected regenerated OSL.

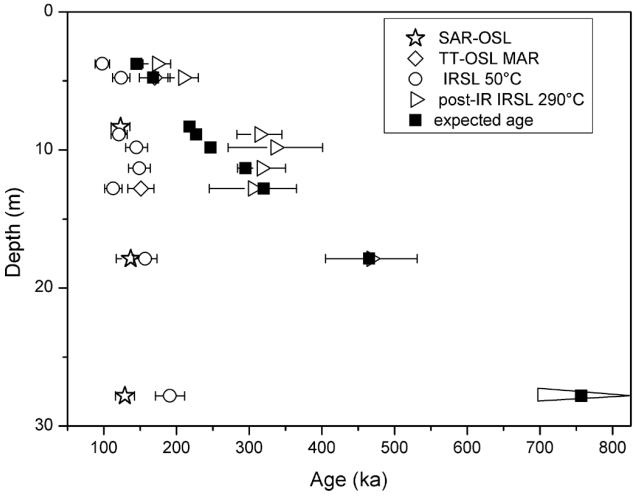

Fig. 6. Comparison of the expected ages from an independent age model (Melles et al., 2012; Nowaczyk et al., 2013) and luminescence ages determined with different luminescence dating protocols on fine grain quartz and on polymineral fine grain. The graph shows the luminescence ages which were calculated with the measured water content. The extended triangle in the lower right corner correlates with the sample from the B/M boundary and is a symbol for the pIRIR$_{290}$ age of > 700 ka.

6.2 TT-OSL

The SAR protocol for TT-OSL developed by Porat et al. (2009) (Table 2) was not suited for the quartz from Lake El'gygytgyn because significant sensitivity changes and a

non-linear dose response prevented the fitting of a dose response curve to the data. Independent tests of the modified TT-OSL protocol (Table 2) with additional hot bleaches applied on a laboratory test quartz with an artificial beta dose of 206 Gy yielded a perfect linear growth curve, a very small underestimation of about 5 %, and a given to measured dose ratio of 1.05. The average recycling ratio was within 10 % deviation and the recuperation was negligible. This result underlines the general validity of the modified TT-OSL protocol, which obviously is not suitable for the samples of this study.

The results obtained by the multiple aliquot approach show linear growth curves and a good response to the short shine normalisation. Sample 1A1H3 delivers an age of 170 ± 21 ka and perfectly matches the expected age range that is inferred from the independent age model. The result of sample 1A4H2, however, underestimates the expected age range significantly (Table 3). Hence, with respect to the independent age control TT-OSL protocols were considered not to yield the required reliability for dating the samples under study here.

6.3 SAR-IRSL at 50 °C

The D_e-values obtained for the standard SAR-IRSL$_{50}$ protocol (Table 2) show a constant increase with depth and the age estimates range from 98 ± 10 ka to a maximum age of 191 ± 20 ka for the sample attributed to the B/M boundary. The mean recycling ratio of all samples is between 0.97 and 0.98 and the reproducibility is excellent (Table 5) but the expected age range is not matched (Table 6). Deconvolution of a dose response curve from sample 1A6H1B shows a similar trend as observed for fine grain quartz. The dose response curve is best fitted to a SEPL function but the sensitivity corrected IRSL signal (L_x) is in saturation (Fig. S2 in the Supplement). The corresponding sensitivity corrected test dose signal (T_x) is decreasing with each regeneration cycle. The quotient results in an apparent increase of the dose response curve, but this is a laboratory artefact. Fading tests were carried out on 2 samples using the protocol based on the fading correction model of Lamothe et al. (2003) and described by Auclair et al. (2003). They revealed small fading rates between of 1.2 ± 0.4 % decade^{-1} (1B3H2) and 0.6 ± 0.4 % decade^{-1} (1A3H1) and suggest age underestimations of about 7–10 % for the standard SAR protocol. Juschus et al. (2007) and Forman et al. (2007) also described very small fading ratios for their polymineral fine grain from younger Lake El'gygytgyn sediments and they forebear from doing fading corrections. They obtained a good agreement with the expected age range up to ∼ 160 ka, but underestimate the expected age range beyond 160 ka (Forman et al., 2007).

6.4 Post-IR IRSL at 290 °C

The results obtained by pIRIR$_{290}$ show increasing D_e-values from 449 ± 30 Gy up to more than 2400 Gy and a non-uniform increase of consequential age estimates. The mean recycling ratio is between 0.94 and 0.98 and recuperation is generally below 1 %. The random standard deviation (RSD) is small but 1A4H2 and 1A3H2 have RSDs of more than 30 %. Deconvolution of a dose response curve from sample 1A6H1B shows a constant growth of the regenerated signal up to 2440 Gy and a continuous increase of the corresponding test dose signal with measuring cycle (Fig. S3 in the Supplement).

Thomsen et al. (2008) and Buylaert et al. (2009) have demonstrated that the pIRIR signal is easy to bleach down to a certain residual level of 10–20 Gy, but that it is necessary to verify this assumption, since bleaching characteristics are strongly dependent on the sediment type and mineralogy of the feldspars. A sample set of 1A1H2 was prepared and bleached for 3.3 h and 7.5 h under natural sunlight on a bright cloudless day in June. Another sample set was bleached in a Höhnle solar simulator for 4.5 h, 6.5 h and 36 h. The results (Table 4) confirm that the pIRIR$_{290}$ signal is generally easy to bleach. After 3.3 h under natural sunlight, the pIRIR$_{290}$ D_e of sample 1A1H2 is already reduced to about 20 Gy and it keeps decreasing with further exposure time. Artificial bleaching of different samples in a Höhnle solar simulator for 4.5, 6.5 h and 36 h gives a residual below 20 Gy. After 36 h in a solar simulator there is still a residual of 12 Gy, but the bleaching level is sample dependent and not only dependent on the bleaching time. However, this experiment illustrates that the pIRIR signal of the lake sediments can be bleached to a reasonable level in a reasonable time.

The impact of these residuals on the calculated ages can be considered to be quite low. For example, the residual of about 20 Gy measured after 3.3 h of sunlight bleaching for sample 1A1H2 (Table 4), corresponds to 7.7 ka using the dose rate based on the measured water content. The pIRIR$_{290}$ age of this sample is 173 ± 19 ka after subtraction of the residual. Thus, the residual correlates to only 4 % of the age and within the range of the 1-sigma error in age.

Dose recovery tests at 1A1H2 after a natural sunlight exposure for 7.5 h and a given dose of ∼ 470 Gy failed to pass the criteria. After subtracting the residual of 14 Gy the measured to given dose ratio was still 1.55 ± 0.09, but a valid protocol should be able to deliver a ratio within 10 % deviation from unity. Another dose recovery test was carried out on five discs of sample 1A3H2 after 390 min light exposure in the solar simulator and an artificial beta dose of ∼ 300 Gy. The measured to given dose ratio was still 1.47 ± 0.08, showing a massive overestimation, too. A further dose recovery test on sample 1A3H1 was carried out after 36 h bleaching in the solar simulator. The sub-samples were stored for 6 months after bleaching, then received a beta dose of ∼ 300 Gy and the average measured to given dose ratio was 1.10 ± 0.02,

Table 4. Results of the pIRIR$_{290}$ bleaching experiments.

Sample ID	Composite depth (m)	Bleaching source	Time (h)	pIRIR$_{290}$ residual (Gy)
1A1H2	6.487–6.587	Sunlight	7.5	13.5 ± 1.4
1A1H2	6.487–6.587	Sunlight	3.3	20.3 ± 1.3
1A3H1	11.694–11.794	Solar simulator	36.0	12.4 ± 0.7
1A3H2	12.596–12.696	Solar simulator	6.5	17.3 ± 1.2
1A9H2	31.05–31.15	Solar simulator	4.5	12.7 ± 2.4

which is within the acceptable 10 % range. Five other discs of sample 1A3H1 and 1A3H2 received a hot bleach in the reader (step 7–10 of the protocol, Table 2) instead of an optical bleach, a beta dose of ~ 300 Gy and were then measured. The measured to given dose ratio was 0.99 ± 0.01 for 1A3H1 and 0.96 ± 0.02 for 1A3H2, thus passing the validity test. The other two routine tests, which are commonly checked by default, gave excellent results, illustrating that the sensitivity correction of the protocol is working well. The average recycling ratio was 1.03 ± 0.02 and the recuperation was low, ranging between 1.0 and 1.5 % of the sensitivity corrected natural signal. The results obtained for the dose recovery tests using optical bleaching immediately followed by a beta dose seem to indicate some kind of charge transfer after irradiation and during the first pre-heat. Although the natural signal is thoroughly bleached after a few hours under natural or artificial sunlight (Table 4), it is not possible to recover a given dose if measured immediately after bleaching. The resulting D_e overestimates the given dose significantly. If the sample is stored for some months after bleaching, the overestimation is reduced and the given dose can be recovered within 10 % deviation. Cleaning out the samples with a hot bleach before the first beta dose yields acceptable dose recovery ratios, suggesting no significant charge transfer or recuperation processes. At this stage, we do not have satisfactory explanation for the different behaviours with and without delay between bleaching and irradiation. We interpret this charge transfer observed after optical bleaching and immediate radiation as a laboratory artefact, which is not relevant for natural samples because under natural conditions bleaching and dosing will happen much slower. However, further experiments with varying pause times between bleaching, artificial irradiation and first pre-heat are necessary to analyse these observations in more detail.

7 Discussion of SAR-IRSL$_{50}$ and pIRIR$_{290}$ results

From the comparison of the luminescence dates with the independent age model it becomes evident that only the pIRIR$_{290}$ protocol yielded reliable dating results significantly beyond 200 ka (Table 6). Six of the samples are in very good agreement with the expected age range, if the measured water content is used for age calculation. The pIRIR$_{290}$ D_e-values (Table 5) show an apparent increase with depth, although there is no real increase of D_e for the samples between 200 and 300 ka. The upper two samples of this time slice (1A3H1 and 1A3H2) overestimate the expected age range by about 30 % (Fig. 6), whereas 1B3H2 and 1A4H2 are in good agreement with age estimates. Many reasons are conceivable for overestimations, such as saturation effects as visible for sample 1A3H2, erroneous water contents or dose rate calculations. Partial bleaching is also a potential source for overestimations in luminescence dating but regarding the sedimentation conditions of the lake (Melles et al., 2007) and former dating studies (Juschus et al., 2007; Lukas et al., 2012) incomplete bleaching is not characteristic for lacustrine sediments. Circulation during the summer months and low suspension loads should enable a reasonable reset of the signal. Rapid mass movements from the lake shore to the lake centre might prevent sufficient bleaching during the sedimentation process since time is short between erosion and re-deposition and the water column is large and loaded with suspended matter. Such turbidite layers can be identified in the sediment core but it is uncertain if the time between initial deposition and the turbidity event can be resolved by luminescence dating since the turbidits mainly consist of near surface material from the shelf and the sediments are probably only a few thousand years older than the final mass moving event (Juschus et al., 2007). However, there was no sedimentological evidence that 1A3H1 or 1A3H2 were taken from a turbidite but 1A1H3 represents a mass movement event and is in good agreement with the expected age.

The samples from the lower part of the profile are in good agreement with the expected age and even sample 1A9H2 from the B/M boundary with an expected natural dose of > 2700 Gy gave a D_e of more than 2400 Gy (Figs. 7 and 8a) and an age of > 700 ka (Fig. 6). The dose response curves are best fitted to an exponential plus linear function and the natural sensitivity corrected signals exceed the highest regenerated dose point of 2430 Gy. The D_e obtained for 1A9H2 lies in the extrapolated part of the dose response curve and the true saturation level was not reached. D_e and age are hence just given as minimum values. In this part of the core section, the natural pIRIR$_{290}$ signal is slowly approaching the saturation level, but the dose response curve is rather steep compared to sample 1A6H1B (Fig. 7) and the relative standard deviation (RSD) of 8 % is low. Saturation dose experiments carried out on sample 1A6H1B and 1A4H2 with up to 7 regeneration dose points and a maximum dose of 2500 Gy still allow fitting an exponential plus linear function to the data but the natural pIRIR$_{290}$ signal lies in the upper slow rising linear part of the dose response curve and is close to saturation. This slow rise considerably limits the reliability of the pIRIR results and is taken as one of the reasons for the comparably large relative standard deviation (Table 5), though it is not observed in all samples. Sample 1B3H2 and 1A9H2 have comparably steep rising curves and a small RSD. Polymineral fine grain samples usually do not show a significant scatter because a large number of grains

Table 5. Equivalent doses obtained for the standard SAR-IRSL$_{50}$ protocol and the pIRIR$_{290}$ protocol.

Sample ID	Composite depth (m)	Number of discs[a]	RSD (%)	IRSL$_{50}$ D_e (Gy)	Number of discs[a]	RSD (%)	pIRIR$_{290}$ D_e (Gy)[b]
1A1H2	6.487–6.587	5/6	4	254 ± 14	4/5	6	449 ± 30
1A1H3	7.469–7.569	6/6	2	343 ± 19	11/13	9	581 ± 34
1A3H1	11.694–11.794	7/7	5	351 ± 19	4/5	5	911 ± 58
1A3H2	12.596–12.696	5/5	3	412 ± 25	5/8	34	958 ± 116
1B3H2	14.169–14.269	7/7	4	414 ± 23	5/5	11	883 ± 56
1A4H2	15.626–15.726	6/6	2	428 ± 24	8/9	32	1158 ± 200
1A6H1B	20.869–20.969	5/6	5	539 ± 33	6/6	16	1605 ± 168
1A9H2	31.05–31.15	6/6	4	645 ± 38	5/5	8	> 2400

[a] Number of discs taken for D_e determination and total number of discs measured. [b] Relating to the bleaching experiments, the residual signal equivalent to 20 Gy was subtracted from the D_e.

Table 6. Results of the standard SAR-IRSL$_{50}$ protocol and the pIRIR$_{290}$ protocol. Ages and dose rates are given for various assumed and the measured water contents. All analytical results are presented with their 1-sigma error.

Sample ID	Composite depth (m)	Expected age (ka)*	IRSL$_{50}$ age (ka) Water content assumed for age calculation				pIRIR$_{290}$ age (ka) Water content assumed for age calculation				Dose rate (Gy ka^{-1}) Water content assumed for age calculation			
			measured	50 %	70 %	90 %	measured	50 %	70 %	90 %	measured	50 %	70 %	90 %
1A1H2	6.487–6.587	~ 145	98 ± 10	74 ± 7	85 ± 8	95 ± 10	173 ± 19	130 ± 13	149 ± 16	169 ± 18	2.6 ± 0.2	3.5 ± 0.3	3.0 ± 0.2	2.7 ± 0.2
1A1H3	7.469–7.569	~ 168	124 ± 12	102 ± 10	117 ± 12	132 ± 14	209 ± 21	172 ± 17	198 ± 20	223 ± 23	2.8 ± 0.2	3.4 ± 0.3	2.9 ± 0.2	2.6 ± 0.2
1A3H1	11.694–11.794	~ 227	121 ± 11	128 ± 12	147 ± 14	166 ± 17	314 ± 31	332 ± 34	381 ± 40	430 ± 46	2.9 ± 0.2	2.7 ± 0.2	2.4 ± 0.2	2.1 ± 0.2
1A3H2	12.596–12.696	~ 247	145 ± 15	122 ± 12	141 ± 14	159 ± 17	337 ± 65	284 ± 54	327 ± 63	369 ± 71	2.8 ± 0.2	3.4 ± 0.3	2.9 ± 0.2	2.6 ± 0.2
1B3H2	14.169–14.269	~ 295	149 ± 15	132 ± 13	151 ± 15	171 ± 17	317 ± 33	281 ± 28	323 ± 33	364 ± 39	2.8 ± 0.2	3.1 ± 0.2	2.7 ± 0.2	2.4 ± 0.2
1A4H2	15.626–15.726	~ 320	113 ± 12	98 ± 10	112 ± 12	127 ± 14	305 ± 60	265 ± 51	304 ± 59	343 ± 67	3.8 ± 0.3	4.4 ± 0.4	3.8 ± 0.3	3.4 ± 0.3
1A6H1B	20.869–20.969	~ 465	157 ± 16	145 ± 15	167 ± 18	188 ± 20	468 ± 63	433 ± 57	497 ± 67	561 ± 77	3.4 ± 0.3	3.7 ± 0.3	3.2 ± 0.3	2.9 ± 0.3
1A9H2	31.05–31.15	~ 757	191 ± 20	176 ± 18	202 ± 21	228 ± 24	> 700	> 650	> 750	> 850	3.4 ± 0.3	3.7 ± 0.3	3.2 ± 0.3	2.8 ± 0.2

* Inferred from Melles et al. (2012) and Nowaczyk et al. (2013).

on the sample disc are emitting luminescence signals. Even if the number of aliquots is small and the validity is limited, this scatter is most likely ascribed to the shape of the dose response curves, indicating a natural dose close to saturation level. The scatter for IRSL measurements at 50 °C is much smaller. However, analyses of the natural dose response curve (L_n/T_n) compared to the laboratory-generated dose response curve, as proposed by Chapot et al. (2012), resulted in good accordance (Fig. 8a) and the average DRC of all individual measurements shows the same trend as the natural dose response curve (Fig. 8b). Chapot et al. (2012) have observed different shapes of the dose response curves and a ceasing growth in equivalent natural L_n/T_n doses compared to L_n/T_n values induced by laboratory doses and took this divergence to determine their maximum dating limit. There are no such differences in shape and growth of the dose response curves for the pIRIR measurements of this study but for IRSL measurements at 50 °C and for quartz OSL measurements. The data obtained for pIRIR$_{290}$ measurements from Lake El'gygytgyn are best fitted to a SEPL function with a R^2-value of 0.99 which is in accordance with the typical laboratory dose response curves (Fig. 8b). The relation between the measured and expected D_e-values also gives a hint to the maximum limit of reliable D_e determination but as shown in Fig. 8a, this limit is not reached yet for the samples from Lake El'gygytgyn. The data set obtained for the IRSL$_{50}$ shows a good curve fit to a SEPL function with a $R^2 = 0.99$ but compared to the laboratory-generated dose response curves, the linear part is less steep and the discrepancy between expected and measured D_e-values is significant (Fig. S4 in the Supplement). The comparison of the natural DRC and the laboratory-generated DRC's indicate a large divergence in shape and growth (Fig. S5 in the Supplement), similar to the observations of Chapot at al. (2012) and explains the large underestimations of the IRSL$_{50}$ results, although the fading rates are extremely low.

A similar dating approach by Thiel et al. (2011) on polymineral fine grains extracted from Austrian loess from below the B/M boundary was not successful because the natural of the pIRIR$_{290}$ signal was in the saturating part of the dose response curve, which they defined as > 1600 Gy. In our study the pIRIR$_{290}$ saturation dose was not reached up to 2400 Gy for sample 1A9H2, which is correlated to the B/M boundary. D_e-values derived for the low temperature IRSL signal (Table 2) do not exceed a maximum value of 645 Gy (Table 5) and a maximum age of 191 ± 20 ka for the lowermost sample. A similar trend was described by Forman et al. (2007), who reported on significant underestimations beyond 160 ka for multiple aliquot low temperature IRSL measurements on polymineral fine grains. Finally, we deduce that the predominant agreement with the age model, the shape of the natural dose response curve and the age increase with

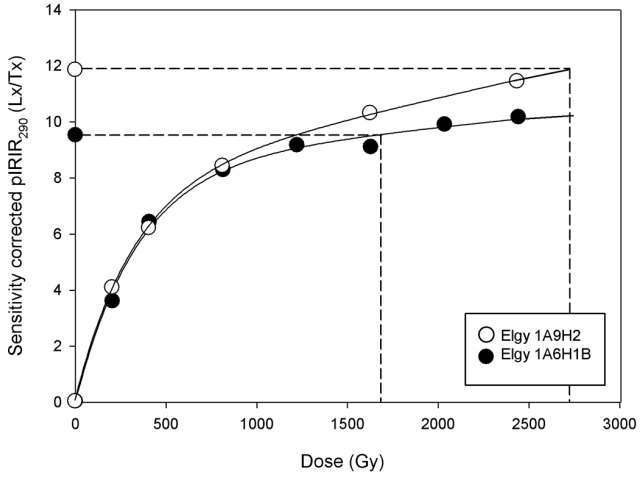

Fig. 7. Dose response curves of the pIRIR$_{290}$ protocol applied to polymineral fine grain extracts of sample 1A6H2B and 1A9H2. The data is best fitted to a single exponential plus linear (SEPL) function. Although sample 1A6H1B is much younger than 1A9H2, the linear part of the DRC is less steep and slowly approaching the saturation level. This results in large errors and substantially limits the precision of pIRIR$_{290}$ D_e determination.

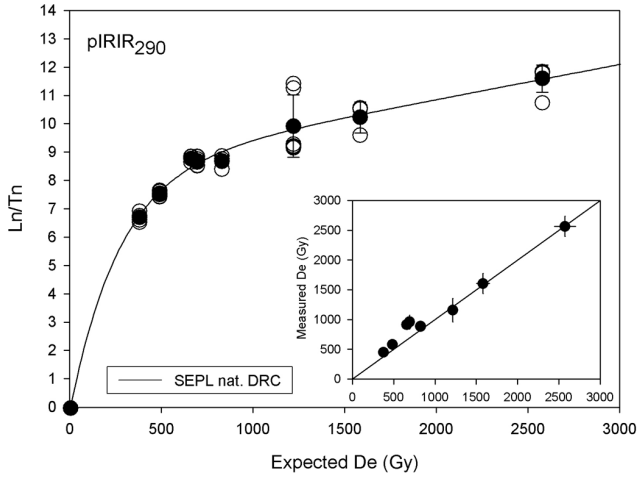

Fig. 8a. Test dose normalised natural optically stimulated luminescence signals (L_n/T_n) of the eight samples used for the pIRIR$_{290}$ protocol plotted against their expected equivalent dose values (D_e) (Chapot et al., 2012). The expected D_e for each sample was calculated by multiplying the environmental dose rate by the expected age. The inset shows the comparably good agreement between the expected and the measured D_e. The solid line is the 1 : 1 line.

depth (Table 6) argue for the validity of the pIRIR$_{290}$ data in this study.

No fading corrections were made, neither for the IRSL$_{50}$ nor the pIRIR$_{290}$ D_e-values. Juschus et al. (2007) reported on small fading ratios between 0.84 and 0.99 and followed Forman et al. (2007), who determined fading ratios between 0.92 and 0.99 and did not apply fading corrections. The

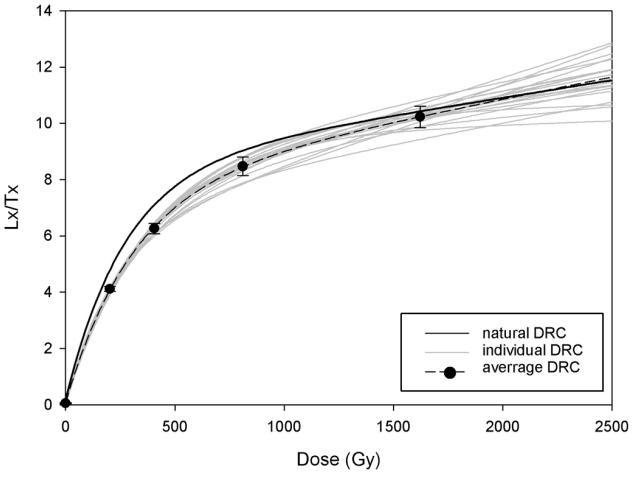

Fig. 8b. Comparison of the natural dose response curve (DRC) from Fig. 8a with the single aliquot regenerative DRCs of the aliquots used to construct the natural DRC.

same trend was observed for two samples from this study, which gave fading rates of 1.2±0.4 % decade^{-1} (1B3H2) and 0.6 ± 0.4 % decade^{-1} (1A3H1) for IRSL$_{50}$. Although these rates are small, an influence cannot be excluded. However, the introduced uncertainties associated with fading corrections in the considered age range are supposed to exceed any advantage of correction here. Buylaert et al. (2012) calculated fading rates for low temperature IRSL and post-IR IRSL at samples of different origins and concluded that fading rates of 1–1.5 % decade^{-1} are most likely artefacts of measurement procedures. We, hence, have decided against conducting any fading corrections for IRSL$_{50}$ and pIRIR$_{290}$ dose estimates.

8 Conclusions

The samples from Lake El'gygytgyn turned out to be very challenging for luminescence dating and the reasons therefore are manifold. Although the general luminescence properties of the sample material, such as signal intensity, recuperation, dose response, sensitivity, and others are acceptable for the fine-grained quartz and polymineral fractions, only one measuring protocol yielded reasonable results with regard to the independent age model. The TT-OSL protocol was inappropriate because insufficient sensitivity corrections prevented a reliable curve fit. A multiple aliquot TT-OSL protocol for fine grain quartz was tested, but failed for the older samples as well. The SAR protocol for OSL and IRSL$_{50}$ dating techniques also failed to deliver satisfactory and reliable dating results. They both underestimate the paleomagnetic time frame significantly, for example date the sample from the 780 ka B/M boundary to only about 130 ka and 190 ka, respectively. A deconvolution of the dose response curves show for both techniques a similar trend of

a decreasing test dose response which results in a pseudo-increase of the dose response curves. This explains the underestimations observed for quartz and polymineral fine grain measured by OSL and $IRSL_{50}$. Large discrepancies between natural and laboratory dose response curves observed for quartz and $IRSL_{50}$ confirm this interpretation and can explain the massive underestimations of the $IRSL_{50}$ signal even though the fading rate is very low.

Only $pIRIR_{290}$ measurements have passed all validation tests and result in ages that increase with depth down to the B/M boundary. The natural and the laboratory generated dose response curves are in perfect accordance, showing that continued signal growth not only appears in the laboratory but also in nature. The deconvolution of a dose response curve shows a constant increase of L_x and the corresponding T_x and the quotient L_x/T_x consequently shows a real and no pseudo-increase with dose. Six out of eight samples are in fairly good agreement with the ages calculated from the magnetic polarity, though their errors are large. However, the upper two samples from the MIS 7 sediment record seem to show overestimations and no increase in age with depth. It is not possible to verify if this overestimation is partly due to insufficient bleaching, turbiditic events, erroneous estimation of water contents or other dosimetric uncertainties. Thus, for verification of the dating results obtained in this study it might be interesting for further projects to analyse the effective bleaching of a modern sample from the delta of one of the small inlet streams of Lake El'gygytgyn.

Supplementary material related to this article is available online at: http://www.clim-past.net/9/719/2013/cp-9-719-2013-supplement.pdf.

Acknowledgements. Funding for the "El'gygytgyn Drilling Project" was provided by the International Continental Scientific Drilling Program (IPDP), the US National Science Foundation, the German Federal Ministry of Education and Research (BMBF; grant 03G0642), Alfred Wegener Institute (AWI) and GeoForschungsZentrum (GFZ), the Russian Academy of Sciences Far East Branch (RAS-FEB), the Russian Foundation for Basic Research (RFBR), and the Austrian Federal Ministry of Science and Research (BMWF). The Russian GLAD 800 drilling system was developed and operated by DOSECC Inc., and LacCore, at the University of Minnesota, handled core curation. Financial support for the luminescence dating was provided by the BMBF. We thank all participants on the drilling operation and on the core sub-sampling at the University of Cologne for their competent help and collaboration. Water content measurements as listed in Table 1 were contributed by V. Wennrich.

Edited by: M. Melles

References

Adamiec, G. and Aitken, M. J.: Dose-rate conversion factors: update, Ancient TL, 16, 37–49, 1998.

Auclair, M., Lamothe, M., and Huot, S.: Measurement of anomalous fading for feldspar IRSL using SAR, Radiat. Meas., 37, 487–492, 2003.

Ballarini, M., Wallinga, J., Wintle, A. G., and Bos, A. J. J.: A modified SAR protocol for optical dating of individual grains from young quartz samples, Radiat. Meas., 42, 360–369, 2007.

Buylaert, J.-P., Murray, A. S., Thomsen, K. J., and Jain, M.: Testing the potential of an elevated temperature IRSL signal from K-feldspar, Radiat. Meas., 44, 560–565, 2009.

Buylaert, J.-P., Jain, M., Murray, A. S., Thomsen, K. J., Thiel, C., and Sohbati, R.: A robust feldspar luminescence dating method for Middle and Late Pleistocene sediments, Boreas, 41, 435–451, 2012.

Chapot, M. S., Roberts, H. M., Duller, G. A. T., and Lai, Z. P.: A comparison of natural- and laboratory-generated dose response curves for quartz optically stimulated luminescence signals from Chinese Loess, Radiat. Meas., 47, 1045–1052, doi:10.1016/j.radmeas.2012.09.001, 2012.

Forman, S. L., Pierson, J., Gomez, J., Brigham-Grette, J., Nowaczyk, N. R., and Melles, M.: Luminescence geochronology for sediments from Lake El'gygytgyn, northeast Siberia, Russia: constraining the timing of paleoenvironmental events for the past 200 ka, J. Paleolimnol., 37, 77–88, 2007.

Frechen, M. and Schirmer, W,: Luminescence Chronology of the Schwalbenberg II Loess in the Middle Rhine Valley, Eiszeitalter und Gegenwart, 60, 78–89, doi:10.3285/eg.60.1.05, 2011.

Frechen, M., Schweitzer, U., and Zander, A.: Improvements in sample preparation for the fine grain technique, Ancient TL, 14, 15–17, 1996.

Gurov, E. P., Koeberl, C., and Yamnichenko, A.: El'gygytgyn impact crater, Russia: structure, tectonics, and morphology, Meteorit. Planet. Sci., 42, 307–319, doi:10.1111/j.1945-5100.2007.tb00235.x, 2007.

Guibert, P., Lahaye, C., and Bechtel, F.: The importance of U-series disequilibrium of sediments in luminescence dating: A case study at the Roc de Marsal Cave (Dordogne, France), Radiat. Meas., 44–3, 223–231, 2009.

Huntley, D. J. and Lamothe, M.: Ubiquity of anomalous fading in K-feldspars and the measurement and correction for it in optical dating, Can. J. Earth Sci., 38, 1093–1106, 2001.

Jacobs, Z., Roberts, R. G., Lachlan, T. J., Karkanas, P., Marean, C. W., and Roberts, D.: Development of the SAR TT-OSL procedure for dating Middle Pleistocene dune and shallow marine deposits along the southern Cape coast of South Africa, Quat. Geochronol., 6, 491–513, 2011.

Juschus, O., Preusser, F., Melles, M., and Radtke, U.: Applying SAR-IRSL methodology for dating fine-grained sediments from Lake El'gygytgyn, north-eastern Siberia, Quat. Geochronol., 2, 187–194, 2007.

Juschus, O., Melles, M., Gebhardt, A. C., and Niessen, F.: Late Quaternary mass movement events in Lake El'gygytgyn, north-eastern Siberia, Sedimentology, 56, 2155–2174, doi:10.1111/j.1365-3091.2009.01074.x, 2009.

Kemski, J., Klingel, A., and Siehl, A.: Die terrestrische Strahlung durch natürliche radioaktive Elemente, Umweltradioaktivität, 69–96, edited by: Siehl, A., Ernst & Sohn, 1996.

Krbetschek, M. R., Rieser, U., Zöller, L., and Heinicke, J.: Radioactive disequilibria in palaeo-dosimetric dating of sediments, Radiat. Meas., 23, 485–489, 1994.

Lai, Z. P.: Chronology and the upper dating limit for loess samples from Luochuan section in the Chinese Loess Plateau using quartz OSL SAR protocol, J. Asian Earth Sci., 37, 176–185, 2010.

Lamothe, M. and Auclair, M.: A solution to anomalous fading and age shortfalls in optical dating of feldspar minerals, Earth Planet. Sc. Lett., 171, 319–323, 1999.

Lamothe, M., Auclair, M., Hamzaoui, C., and Huot, S.: Towards a prediction of longterm anomalous fading of feldspar IRSL, Radiat. Meas., 37, 493–498, 2003.

Li, B. and Li, S. H.: Luminescence dating of K-feldspar from sediments: a protocol without anomalous fading correction, Quat. Geochronol., 6, 468–479, 2011.

Lowick, S. and Preusser, F.: A method for retrospectively calculating water content for desiccated core samples, Ancient TL, 27, 9–14, 2009.

Lowick, S. and Preusser, F.: Investigating age underestimation in the high dose region of optically stimulated luminescence using fine grain quartz, Quat. Geochronol., 6, 33–41, 2011.

Lowick, S., Preusser, F., Pini, R., and Ravazzi, C.: Underestimation of fine grain quartz OSL dating towards the Eemian: Comparison with palynostratigraphy from Azzano Decimo, northeastern Italy, Quat. Geochronol., 5, 583–590, 2010.

Lukas, S., Preusser, F., Anselmetti, D. S., and Tinner, W.: Testing the potential of luminescence dating of high-alpine lake sediments, Quat. Geochronol., 8, 23–32, 2012.

Mauz, B., Packman, S., and Lang, A.: The alpha effectiveness in silt-sized quartz: New data obtained by single and multiple aliquot protocols, Ancient TL, 24, 47–52, 2006.

Melles, M., Brigham-Grette, J., Glushkova, O. Y., Minyuk, P. S., Nowaczyk, N. R., and Hubberten, H.-W.: Sedimentary geochemistry of core PG1351 from Lake El'gygytgyn – a sensitive record of climate variability in the East Siberian Arctic during the past three glacialinterglacial cycles, J. Paleolimnol., 37, 89–104, 2007.

Melles, M., Brigham-Grette, J., Minyuk, P., Koeberl, C., Andreev, A., Cook, T., Fedorov, G., Gebhardt, C., Haltia-Hovi, E., Kukkonen, M., Nowaczyk, N., Schwamborn, G., Wennrich, V., and the El'gygytgyn Scientific Party: The Lake El'gygytgyn scientific drilling project – conquering Arctic challenges through continental drilling, Scientific Drilling, 11, 29–40, doi:10.2204/iodp.sd.11.03.2011, 2011.

Melles, M., Brigham-Grette, J., Minyuk, P. S., Nowaczyk, N. R., Wennrich, V., DeConto, R. M., Anderson, P. M., Andreev, A. A., Coletti, A., Cook, T. L., Haltia-Hovi, E., Kukkonen, M., Lozhkin, A. V., Rosén, P., Tarasov, P., Vogel, H., and Wagner, B.: 2.8 Million Years of Arctic Climate Change from Lake El'gygytgyn, NE Russia, Science, 337, 315–320, doi:10.1126/science.1222135, 2012.

Murray, A. S. and Wintle, A. G.: Luminescence dating of quartz using an improved single-aliquot regenerative-dose protocol, Radiat. Meas., 32, 57–73, 2000.

Murray, A. S., Buylaert, J. P., Henriksen, M., Svendsen, J. I., and Mangerud, J.: Testing the reliability of quartz OSL ages beyond the Eemian, Radiat. Meas., 43, 776–780, 2008.

Niessen, F., Gebhardt, A. C., Kopsch, C., and Wagner, B.: Seismic investigation of the El'gygytgyn impact crater lake (Central Chukotka, NE Siberia): preliminary results, J. Paleolimnol., 37, 17–35, doi:10.1007/s10933-006-9022-9, 2007.

Nolan, M. and Brigham-Grette, J.: Basic hydrology, limnology, and meteorology of modern Lake El'gygytgyn, Siberia, J. Paleolimnol., 37, 17–35, doi:10.1007/s10933-006-9020-y, 2007.

Nolan, M., Liston, G., Prokein, P., Brigham-Grette, J., Sharpton, V., and Huntzinger, R.: Analysis of lake ice dynamics and morphology on Lake El'gygytgyn, Siberia, using SAR and Landsat, J. Geophys. Res., 108, 8162, doi:10.1029/2001JD000934, 2002.

Nowaczyk, N. R., Minyuk, P., Melles, M., Brigham-Grette, J., Glushkova, O. Y., Nolan, M., Lozhkin, A. V., Stetsenko, T. V., Andersen, P. M., and Forman, S. L.: Magnetostratigraphic results from impact crater lake El'gygytgyn, Northeastern Siberia: a possibly 300 kyr long terrestrial paleoclimate record from the Arctic, Geophys. J. Int., 150, 109–126, doi:10.1046/j.1365-246X.2002.01625.x, 2002.

Nowaczyk, N. R., Wennrich, V., Melles, M., Brigham, J., and El'gygytgyn Scientific Party: Detailed age model for upper 125 m of core D1 from Lake El'gygytgyn, NE Russia, as derived from orbital forcing, Clim. Past Discuss., in preparation, 2013.

Porat, N., Duller, G. A. T., Roberts, H. M., and Wintle, A. G.: A simplified SAR protocol for TT-OSL, Radiat. Meas., 44, 538–542, 2009.

Preusser, F. and Degering, D,: Luminescence dating of the Niedeweningen mammoth site, Switzerland, Quaternary Int., 164–165, 106–112, doi:10.1016/j.quaint.2006.12.002, 2007.

Rees-Jones, J.: Optical dating of young sediments using fine-grain quartz, Ancient TL, 13, 9–14, 1995.

Schwamborn, G., Foerster, A., Diekmann, B., Schirrmeister, L., and Fedorov, G.: Mid- to Late-Quaternary Cryogenic Weathering Conditions at El'gygytgyn Crater, Northeastern Russia: Inference from Mineralogical and Microtextural Properties of the Sediment Record, Ninth International Conference On Permafrost, Fairbanks, 1601–1606, 2008.

Schwamborn, G., Fedorov, G., Ostanin, N., Schirrmeister, L., Andreev, A., and the El'gygytgyn Scientific Party: Depositional dynamics in the El'gygytgyn Crater margin: implications for the 3.6 Ma old sediment archive, Clim. Past, 8, 1897–1911, doi:10.5194/cp-8-1897-2012, 2012.

Stevens, T., Buylaert, J.-P., and Murray, A. S.: Towards development of a broadly-applicable SAR TT-OSL dating protocol for quartz, Radiat. Meas., 44, 639–645, 2009.

Thiel, C., Buylaert, J.-P., Murray, A. S., Terhorst, B., Hofer, I., Tsukamoto, S., and Frechen, M.: Luminescence dating of the Stratzing loess profile (Austria) – Testing the potential of an elevated temperature post-IR IRSL protocol, Quaternary Int., 234, 23–31, 2011.

Thomsen, K. J., Murray, A. S., Jain, M., and Bøtter-Jensen, L.: Laboratory fading rates of various luminescence signals from feldspar-rich sediment extracts, Radiat. Meas., 43, 1474–1486, 2008.

Timar, A., Vandenberghe, D., Panaiotu, E. C., Panaiotu, C. G., Necula, C., Cosma, C., and Van den Haute, P.: Optical dating of Romanian loess using fine-grained quartz, Quat. Geochronol., 5, 143–148, 2010.

Treshnikov, A. F.: Atlas of the Arctic, Main Department of Geodesy and Cartography under the Council of Ministers of the USSR, Moscow, 1985.

Tsukamoto, S., Duller, G. A. T., and Wintle, A. G.: Characteristics of thermally transferred optically stimulated luminescence (TT-OSL) in quartz and its potential for dating sediments, Radiat. Meas., 43, 1204–1218, 2008.

Wallinga, J., Murray, A. S., and Wintle, A. G.: The single aliquot regenerative-dose (SAR) protocol applied to coarse-grain feldspar, Radiat. Meas., 32, 529–533, 2000.

Wang, X. L., Wintle, A. G., and Lu, Y. C.: Thermally transferred luminescence in fine-grained quartz from Chinese loess: Basic observations, Radiat. Meas., 41, 649–658, 2006.

Wang, X. L., Wintle, A. G., and Lu, Y. C.: Testing a single-aliquot protocol for recuperated OSL dating, Radiat. Meas., 42, 380–391, 2007.

Wennrich, V., Minyuk, P., Borkhodoev, V., Francke, A., Ritter, B., Raschke, U., Nowaczyk, N., Schwamborn, G., Brigham-Grette, J., Melles, M., and El'gygytgyn Science Party: Pliocene to Pleistocene climate and environmental history of Lake El'gygytgyn / NE Russia based on high-resolution inorganic geochemistry data, Clim. Past Discuss., in preparation, 2013.

Wintle, A. G.: Anomalous fading of thermoluminescence in mineral samples, Nature, 245, 143–144, 1973.

Wintle, A. G. and Murray, A. S.: A review of quartz optically stimulated luminescence characteristics and their relevance in single-aliquot regeneration dating protocols, Radiat. Meas., 41, 369–391, doi:10.1016/j.radmeas.2005.11.001, 2006.

Zander, A., Degering, D., Preusser, F., Kasper, H. U., and Brückner, H.: Optically stimulated luminescence dating of sublittoral and intertidal sediments from Dubai, U.A.E.: Radioactive disequilibria in the uranium decay series, Quat. Geochronol., 2, 123–128, doi:10.1016/j.quageo.2006.04.003, 2007.